Supporting information

Biochemical and Biophysical Analysis of a Chiral PqsD Inhibitor Revealing Tight-binding Behavior and Enantiomers with Contrary Thermodynamic Signatures

Michael P. Storz,[†] Christian Brengel,[†] Elisabeth Weidel,[¶] Michael Hoffmann,[§] Klaus Hollemeyer,[#] Anke Steinbach,[†] Rolf Müller,[§] Martin Empting,[†*] Rolf W. Hartmann[†¶*]

[†] Helmholtz-Institute for Pharmaceutical Research Saarland (HIPS), Department Drug Design and Optimization, Campus $C2_3$, 66123 Saarbrücken, Germany;

[¶] Pharmaceutical and Medicinal Chemistry, Saarland University, Campus $C2_3$, 66123 Saarbrücken, Germany;

[§] Helmholtz-Institute for Pharmaceutical Research Saarland (HIPS), Department Microbial Natural Products, Campus $C2_3$, 66123 Saarbrücken, Germany.

[#] Biochemical Engineering, Saarland University, Campus $A1_5$, 66123 Saarbrücken, Germany.

[‡] These authors contributed equally to this work

Contents:

1) Primer Sequence of Mutations

Mutant	Primer	
	forward 5' → 3'	**reverse 3' →5'**
S317F	GCTGGTCCTGACCTACGGTTTTGGC GCGACCTGGGGCG	CGCCCCAGGTCGCGCCAAAACCGTA GGTCAGGACCAGC
C112A	GCTGGATATCCGGGCACAGGCGAG CGGGTTGCTGTACG	CGTACAGCAACCCGCTCGCCTGTGC CCGGATATCCAGC
H257F	CGACCATGTGATCTGCTTTCAACCG AACCTGC	GCAGGTTCGGTTGAAAGCAGATCAC ATGGTCG
C112S	GCTGGATATCCGGGCACAGAGCAG CGGGTTGCTGTACG'	CGTACAGCAACCCGCTGCTCTGTGC CCGGATATCCAGC
S317A	GCTGGTCCTGACCTACGGTGCGGG CGCGACCTGGGGCG	CGCCCCAGGTCGCGCCCGCACCGT AGGTCAGGACCAGC
N287A	CGTCTGGGCGCGATGGCTTCGGCC	GGCCGAAGCCATCGCGCCCAGACG

2) Table S1: Catalytic Activity of PqsD Wild-type and Mutants[a]

	wild-type	**S317F**	**C112A**	**H257F**	**C112S**	**S317A**	**N287A**
Formed HHQ [nM]	2154	15	1	18	171	2182	7

[a]Reactions were performed according to the screening assay procedure described in the Methods Section using 1.0 µM of *P. aeruginosa* PqsD.

3) Synthesis of Substrates Used in the Enzymatic Inhibition Assays

Synthesis of anthraniloyl-S-CoA thioester *(SI1)*. Anthraniloyl-CoA (ACoA) was synthesized from isatoic anhydride and coenzyme A (CoA) using a previously described method. ACoA was purified by HPLC (Agilent 1200 series consisting of a quaternary pump, a fraction collector and an MWD; Agilent Technologies) after freeze drying of the aqueous reaction mixture (25 ml) and resuspending of the dried residue in 3 ml of a mixture of 50% methanol and water (*v*/*v*). A 10 µm RP C18 150-30 column (30 x 100 mm, Agilent) was used along with a mobile phase consisting of water containing 1‰ TFA (A) and acetonitrile containing 1‰ TFA (B) with a flow rate of 5 ml min^{-1}. The following gradient was used: 0–35 min, linear gradient 10% – 100% B (*v*/*v*); 35–42 min, 100% B; 42–43 min, 10% B (*v*/*v*) (initial conditions). ACoA containing fractions were pooled and freeze dried.

Synthesis of *β*-ketodecanoic acid *(SI2)*. Ethyl 3-oxodecanoate (300 mg, 1.4 mmol) was stirred with NaOH (56 mg, 1.4 mmol) in 2 ml of water overnight. Any remaining ester was removed by washing with Et_2O (10 ml). The aqueous layer was cooled and acidified with 32% HCl (*w*/*v*) to pH = 6. After filtration the 3-oxodecanoic acid was dried *in vacuo* and obtained as white solid (100 mg, 38%). ^{1}H-NMR (500 MHz, $CDCl_3$) δ 0.86 (t, J = 7.0, 3H), 1.25–1.29 (m, 8H), 1.58 (m, 2H), 2.54 (t, J = 7.5, 2H), 3.49 (s, 2H). LC/MS (ESI) *m/z* 242.0, 99% (UV).

Synthesis of ethyl 3-oxodecanoate *(SI3)*. To a THF solution of 2 M LDA (20 ml, 40 mmol) was added ethyl acetoacetate (2.16 g, 16.6 mmol) at 0°C. The deep yellow clear solution was stirred at 0°C for 1 h. To this solution the 1-iodohexane was added (4.20 g, 19.81 mmol) at -78°C. The temperature was allowed to reach an ambient temperature over 14 h and the solution was stirred at room temperature for 2 h. To the solution was added 200 ml of 10% HCl (v/v) and the mixture was extracted with Et_2O (4 × 250 ml). The combined organic layers were dried over Na_2SO_4, filtered, and the filtrate was concentrated *in vacuo*. The residue was purified by column chromatography (*n*-hexane/ethyl acetate, 30/1) to give ethyl 3-oxodecanoate as a yellow oil

(1.98 g, 55%). ^{1}H-NMR (500 MHz, $CDCl_3$) δ 0.84 (t, J = 7.0, 3H), 1.23–1.28 (m, 11H), 1.54 (m, 2H), 2.49 (t, J = 7.0, 2H), 3.39 (s, 2H), 4.16 (m, 2H). LC/MS (ESI) *m/z* 458.0, 87% (UV).

4) Table S2: Comparison of IC_{50} Values Determined by Different Assay Procedures

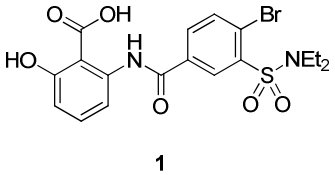

1

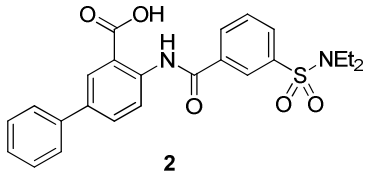

2

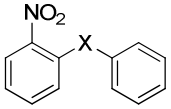

3 X = CHOH
4 X = CHOMe
5 X = SO_2

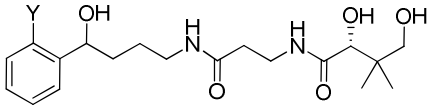

6 Y = NH_2
7 Y = NO_2

Compd	IC_{50} [µM][ab]	$IC_{50,mod}$ [µM][ac]	$IC_{50,ext}$ [µM][ad]
1	1.2 ± 0.1	1.1 ± 0.2	1.8 ± 0.4
2	3.0 ± 0.7	4.2 ± 0.3	7.6 ± 1.5
3	3.2 ± 0.1	24.6 ± 6.2	1.0 ± 0.4
4	4.3 ± 1.0	19.7 ± 8.9	2.6 ± 0.5
5	14.8 ± 2.9	>50	9.7 ± 1.4
6	n.i.	n.d.	n.d.
7	7.9 ± 0.7	n.d.	n.d.

[a]*P. aeruginosa* PqsD (0.1 µM), recombinantly expressed in *Escherichia coli*; anthraniloyl-CoA (5 µM), and *β*-ketodecanoic acid (70 µM); n.i. no inhibition (<10% at 50 µM); n.d. not determined. [b]PqsD and inhibitor were preincubated for 10 min prior to addition of the substrates. [c]Modified procedure including additional preincubation of enzyme and ACoA. [d]Preincubation time of PqsD/inhibitors was extended to 30 min.

5) Percentages of Inhibition and Uncertainty of the Time Dependency Experiment

Compound **2**:

time	control [%]	Cmpd. 2, 3 µM [%]	uncertainty [%]
3 min	100	60.37	2.95
6 min	100	59.36	8.27
9 min	100	60.21	8.09
12 min	100	58.95	8.34
15 min	100	61.99	8.16
20 min	100	72.15	5.19
25 min	100	63.28	7.17
30 min	100	64.18	10.05

Compound **3**:

time	control [%]	Cmpd. 3, 6 µM [%]	uncertainty [%]
3 min	100	71.17	4.33
6 min	100	46.38	2.91
9 min	100	41.85	4.49
12 min	100	36.40	4.36
15 min	100	31.98	4.58
20 min	100	25.39	2.41
25 min	100	27.01	3.60
30 min	100	26.07	4.82

Table S3. HHQ formation in presence of compounds **2** and **3** relative to untreated control.

6) Figure S1: Dose-response Curve of PqsD Inhibition by Compound 3

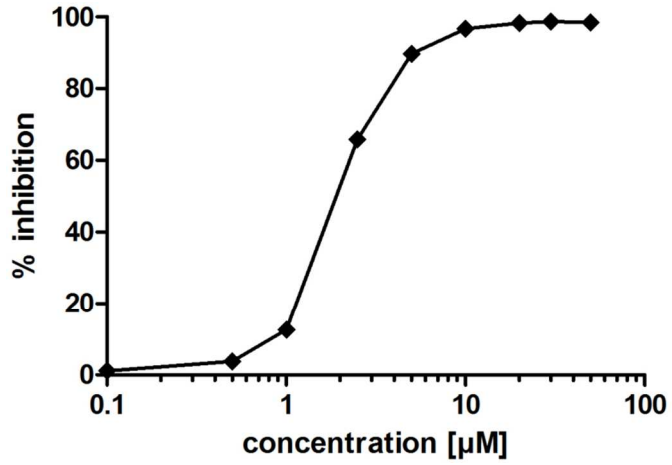

Figure S1. Inhibition of PqsD by compound **3** is plotted against the concentration (log scale). Data were generated using the screening assay procedure for *in vitro* PqsD inhibition as described above. Compounds **4** and **5** show similar curve shapes (data not shown).

7) Further HPLC-ESI MS Experiments

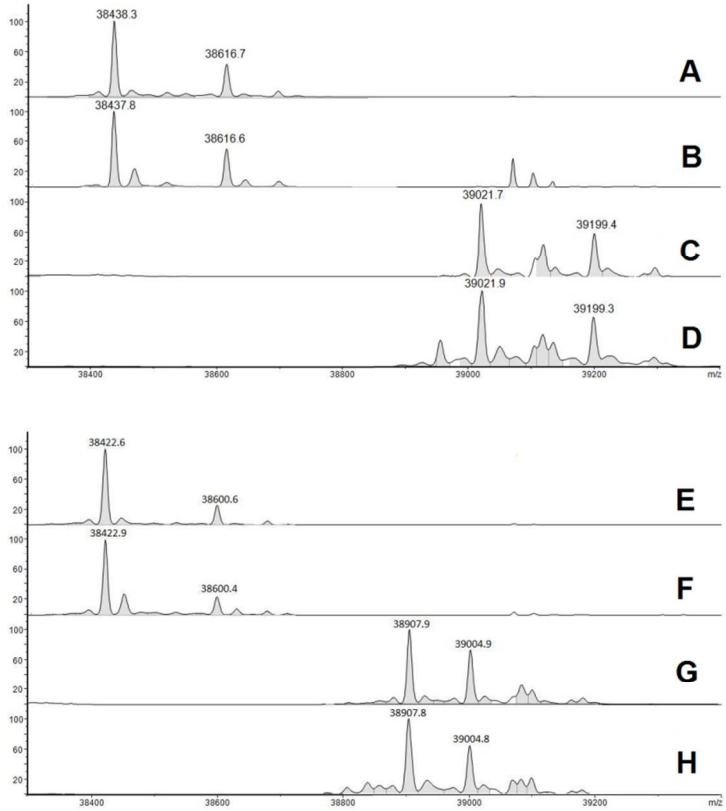

Figure S2. (A-D) PqsD containing a His_6-tag was incubated in absence (A) or in presence (B) of compound **3**. Thereby, no anti-oxidative reagent was present. Samples were subjected to HPLC-ESI MS analysis, whereas no relevant amounts of oxidation products were observed. Subsequent addition of an excess of maleimid resulted in a shift of +582 (corresponding to a 6-fold addition of the labeling agent regardless of the presence of compound **3** (C: PqsD; D: PqsD pretreated with compound **3**). Maleimid labels all available cystein residues present in PqsD, indicating that no cystein was oxidized previously. (E-H) C112S mutant containing a His_6-tag was treated in absence (E) or in presence (F) of compound **3** using the same procedure as described above. Subsequent addition of an excess of maleimid resulted in a shift of +485 (corresponding to a 5-fold addition of the labeling agent regardless of the presence of compound **3** (G: PqsD; H: PqsD pretreated with compound **3**). In all spectra, signals with a shift of +178 Da were observed. This is probably due to spontaneous *α-N*-6-Phosphogluconoylation of the His_6-tag in *E. coli* (SI4).

8) Maldi-TOF Analysis

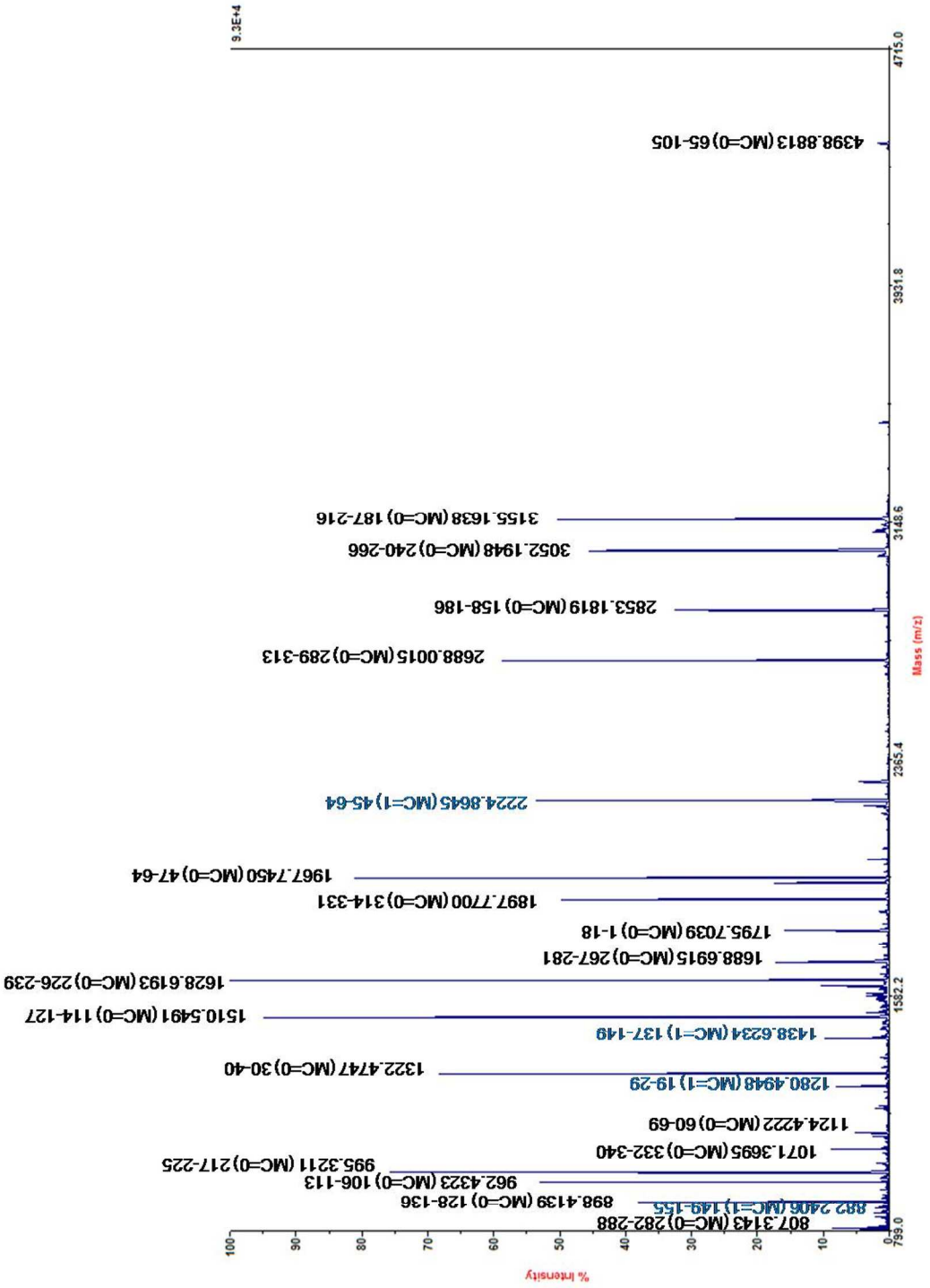

Figure S3. Maldi-TOF spectra of PqsD after tryptic digestion. The blue labeled fragments bear one missed cleavage (*MC*). Fragments generated by complete digestion (*MC*=0) are labeled in black. Together, 334 of 340 amino acids are visible in at least one fragment.

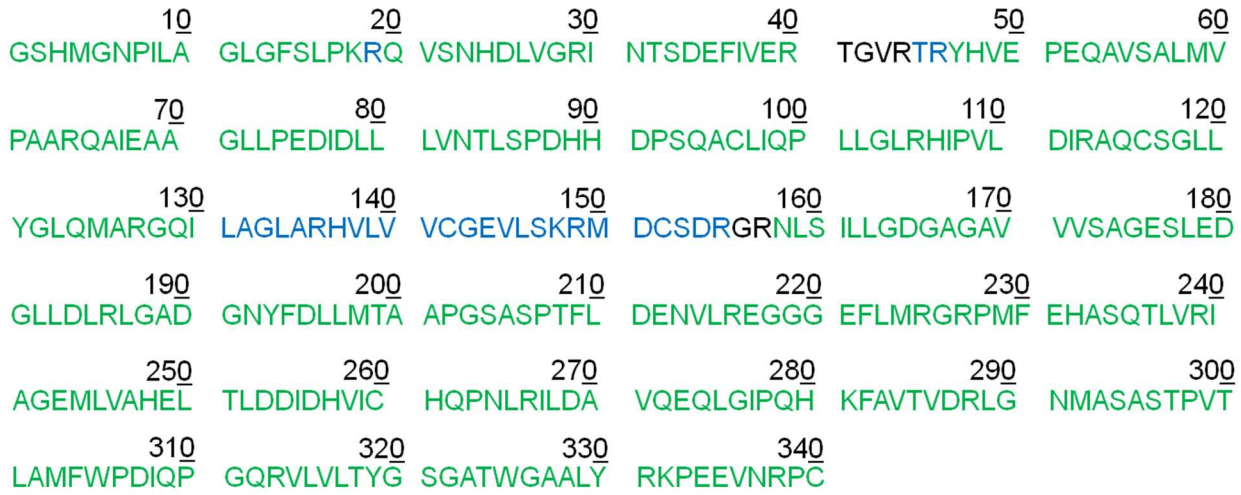

Figure S4. Sequence of the PqsD construct used in the study. Green and blue letters represent amino acids, which are present in peptides (*MC*=0 and *MC*=1, respectively) observed by Maldi-TOF, when native PqsD has been digested. Together, 334 of 340 amino acids are visible in at least one fragment. Amino acids not observed in the experiment are Thr41, Gly42, Val43, Arg44, Gly156 and Arg157. (Numbering refers to the amino acid sequence used in the experiment; in the X-ray structure denoted as Thr37, Gly38, Val39, Arg40, Gly152, Arg153 *(SI5).)*

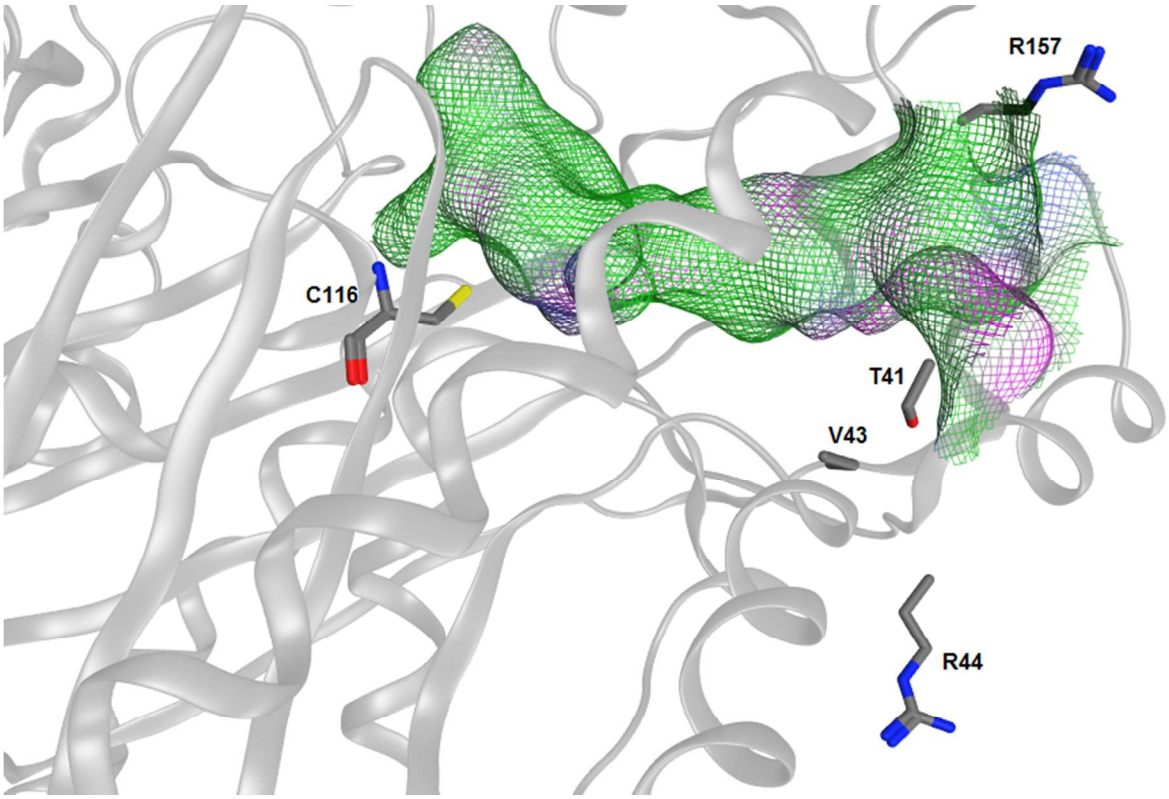

Figure S5. Molecular surface of the PqsD binding channel and side chains of the uncaptured amino acids Thr41, Gly42, Val43, Arg44, Gly156 and Arg157. The alkyl residues of Gly42, Val43 and Gly156 are unable to form covalent bonds. Thr41, Arg44 and Arg157 are located at the tunnel entrance, too far away from the binding site of compound **3**, which is located deep in the active site near the catalytically active Cys116 (in the construct used for X-ray analysis denoted as Cys112).

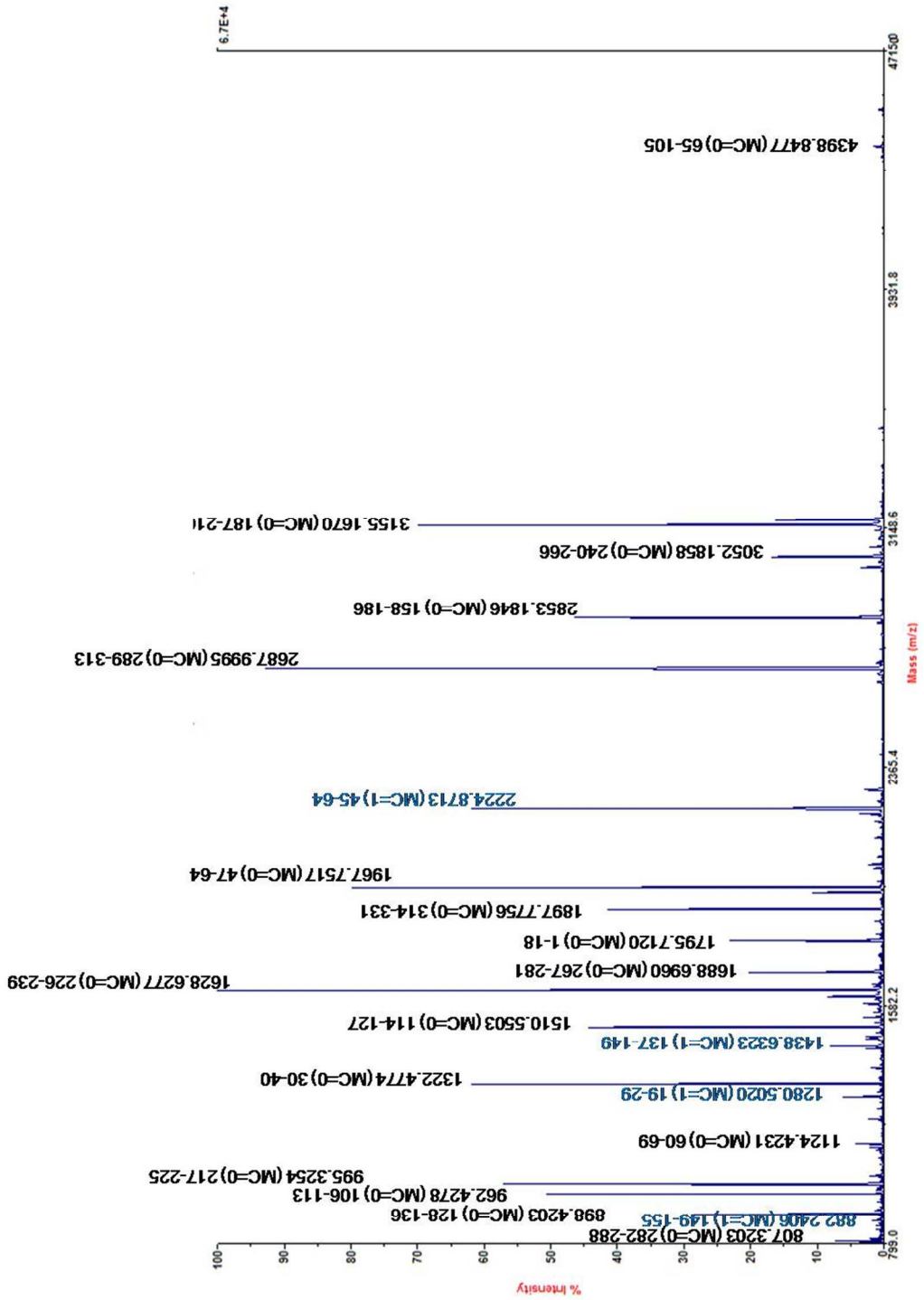

Figure S6. Maldi-TOF spectra of PqsD/compound **3** after tryptic digestion. The blue labeled fragments bear one missed cleavage (*MC*). Fragments generated by complete digestion (*MC*=0) are labeled in black. Compared to untreated PqsD the only difference is the disappearance of the peptide *m*/*z* of 1071.

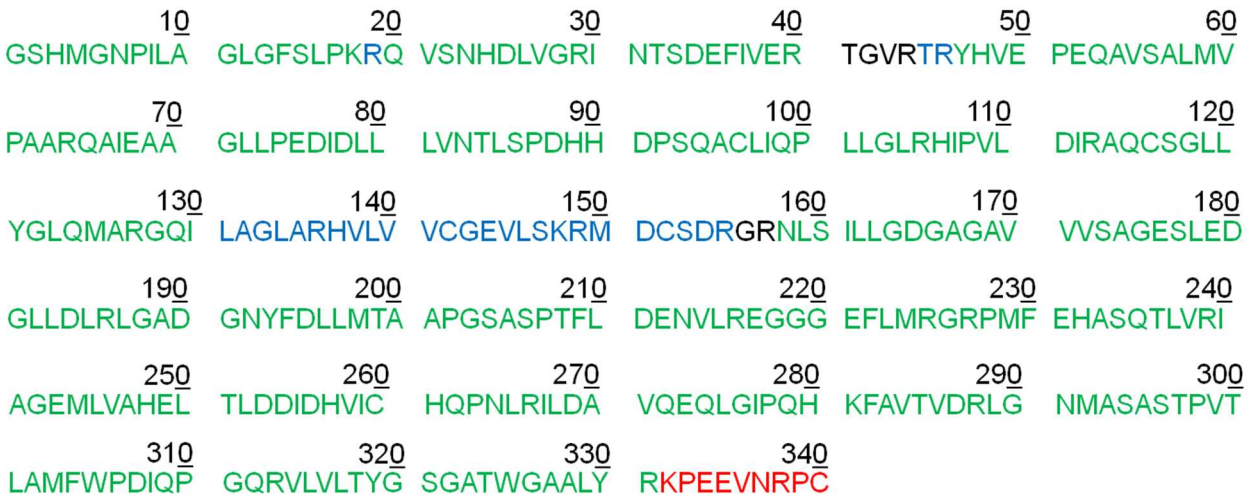

Figure S7. Amino acids observed after preincubation of PqsD with compound **3**. Compared to untreated PqsD the red labeled peptide at the *C*-terminus disappeared, maybe because of an oxidation of the terminal Cys340.

m/z (PqsD) calculated	*m/z* (PqsD) measured	*m/z* (PqsD+ cmpd. 3) measured	Position (Number of missed cleaves)	peptide sequence
4399.3329	4398.8813	4398.8477	65–105 (*MC*=0)	QAIEAAGLLPEDIDLLLVNTLSPDH HDPSQACLIQPLLGLR
3155.5353	3155.1638	3155.1670	187–216 (*MC*=0)	LGADGNYFDLLMTAAPGSASPTF LDENVLR
3052.5342	3052.1948	3052.1858	240–216 (MC=0)	IAGEMLVAHELTLDDIDHVI**CH**QP NLR
2853.5203	2853.1819	2853.1846	158–186 (*MC*=0)	NLSILLGDGAGAVVVSAGESLED GLLDLR
2688.3272	2688.0015	2687.9995	289–313 (*MC*=0)	LGNMASASTPVTLAMFWPDIQPG QR
2225.1495	2224.8645	2224.8713	45–64 (*MC*=1)	TRYHVEPEQAVSALMVPAAR
1968.0007	1967.7450	1967.7517	47–64 (*MC*=0)	YHVEPEQAVSALMVPAAR
1898.0170	1897.7700	1897.7756	314–331 (*MC*=0)	VLVLTYGSGATWGAALYR
1795.9523	1795.7039	1795.7120	1–18 (*MC*=0)	GSHMGNPILAGLGFSLPK
1688.9329	1688.6915	1688.6960	267–281 (*MC*=0)	ILDAVQEQLGIPQHK
1628.8325	1628.6193	1628.6277	226–239 (*MC*=0)	GRPMFEHASQTLVR
1510.7505	1510.5491	1510.5503	114–127 (*MC*=0)	AQCSGLLYGLQMAR
1438.8198	1438.6234	1438.6323	137–149 (*MC*=1)	HVLVVCGEVLSK
1322.6586	1322.4747	1322.4774	30–40 (*MC*=0)	INTSDEFIVER
1282.7187	-	-	137–148 (*MC*=0)	HVLVVCGEVLSK
1280.6818	1280.4948	1280.5020	19–29 (*MC*=1)	RQVSNHDLVGR
1124.5807	1124.4222	1124.4231	60–69 (*MC*=0)	QVSNHDLVGR
1071.5251	1071.3695	-	332–340 (*MC*=0)	KPEEVNRPC
995.4615	995.3211	995.3254	217–225 (*MC*=0)	EGGGEFLMR
962.5781	962.4323	962.4278	106–113 (*MC*=0)	HIPVLDIR
898.5468	898.4139	898.4203	128–136 (*MC*=0)	GQILAGLAR

882.3556	882.2406	882.2174	149–155 (*MC*=1)	RMDCSDR
807.4359	807.3143	807.3203	282–288 (*MC*=0)	FAVTVDR

Table S4. Comparison of peptide masses (calculated and observed by Maldi-TOF analysis) formed by tryptic digestion of untreated PqsD and PqsD treated with compound **3**. All fragments without missed cleavages (*MC*=0) with *m*/*z* >800 are listed. Fragments with *MC*=1 contributing to coverage of the amino acid sequence are added in blue.

9) Separation of 3 into the Enantiomers (*R*)-3 and (*S*)-3 by Chiral-HPLC

The separation was performed using an Agilent 1200 HPLC system equipped with an MWD triggering an automated fraction collector (Agilent Technologies) in "time based" mode. ChemStation® software was used for control and report. The sample was manually injected. A Chiralpak IE® 5µm (250 / 10 mm) column (DAICEL Corporation) was used as stationary phase. The solvent system consisted of *n*-hexane (A) and *iso*-propanol (B). HPLC-Method: Flow rate 2.4 ml min^{-1}. Isocratic run of 7% of B in A (*v*/*v*).

Determination of enantiomeric excess was performed using a Chiralpak IE® 5µm (250 / 4.6 mm) column (DAICEL Corporation) as stationary phase. The solvent system consisted of *n*-heptane (A) and *iso*-propanol (B). HPLC-Method: Flow rate 1 ml min^{-1}. Isocratic run of 7% of B in A (*v*/*v*). The % ee of (*R*)-**9** and (*S*)-**9** was determined using the relative peak areas in the MWD trace.

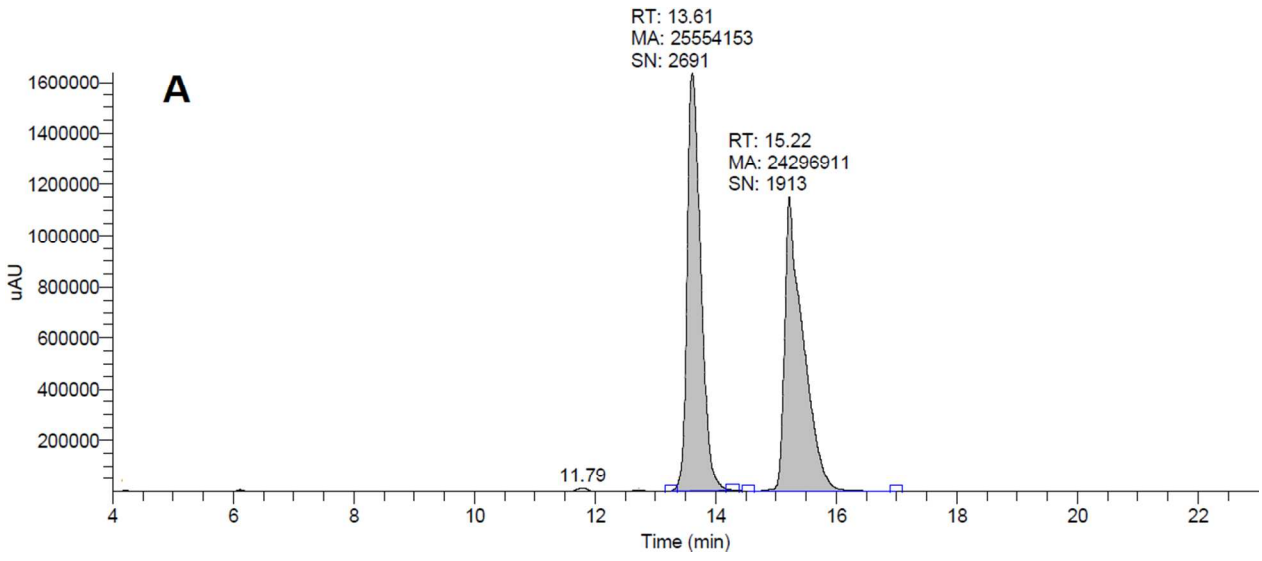

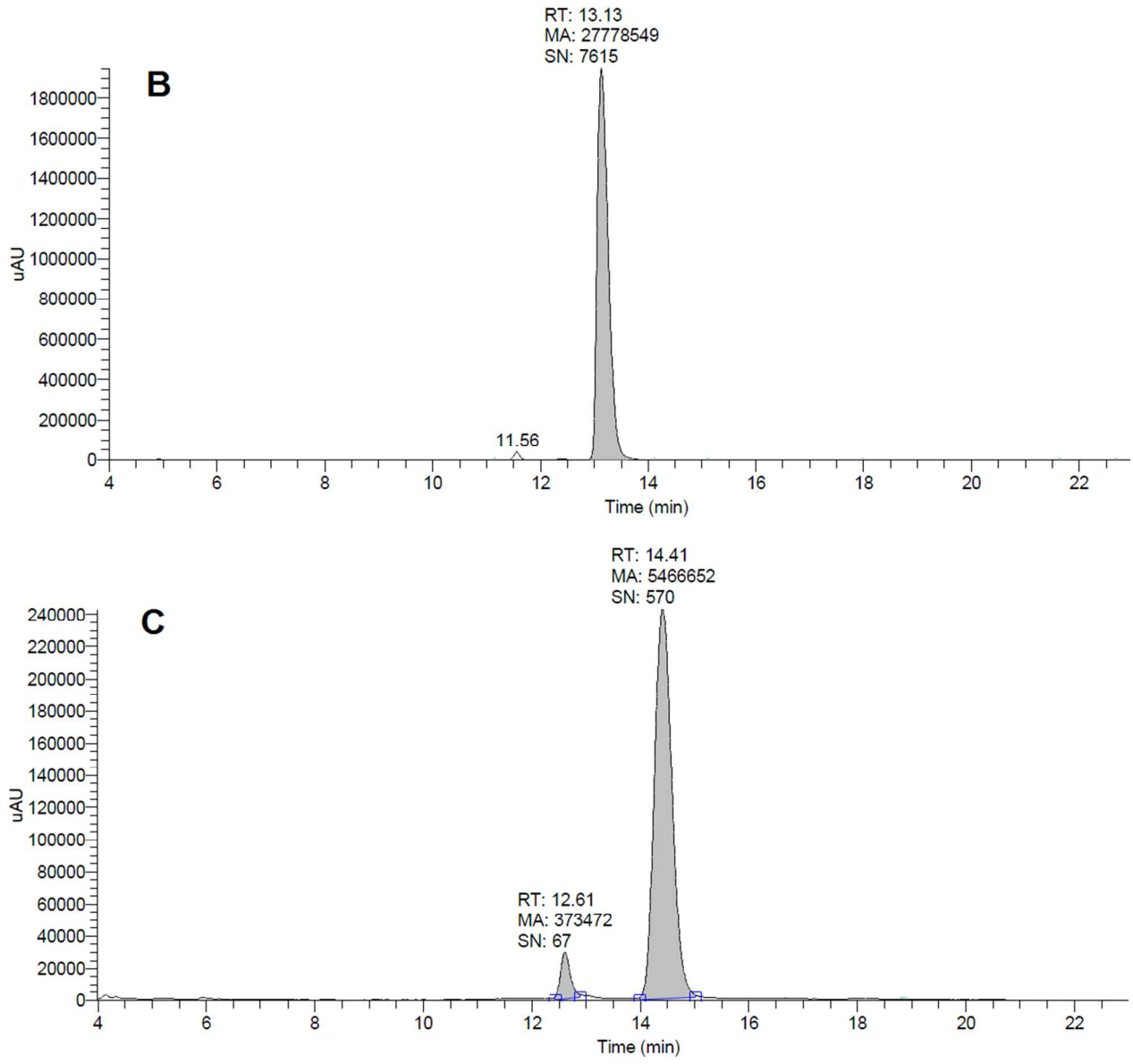

Figure S8. HPLC analysis of enantiomeric purity. (A) Racemic mixture **9**, (B) *S*-enantiomer (–) of **9** (>99.9% ee) and (C) *R*-enantiomer (+) of **9** (87.2% ee). Absolute configurations were derived from measurement of the optical rotation and comparison to literature *(SI6)*.

10) Figure S9: Binding site analysis of (*R*)-3 and (*S*)-3 by SPR

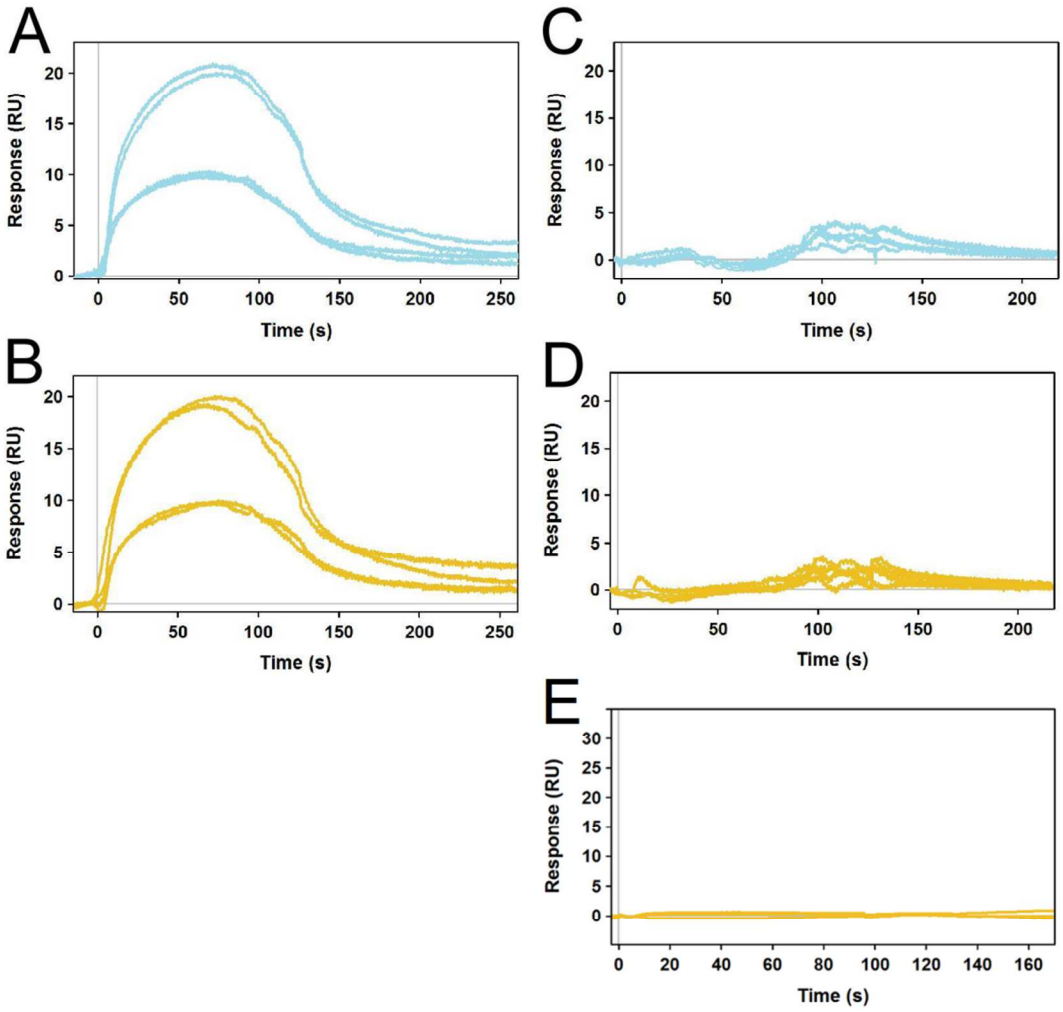

Figure S9. SPR experiment using 250 and 125 µM of (*R*)-**3** (blue) or (*S*)-**3** (orange), respectively. Compounds were added to native PqsD and response curves (A) and (B) were recorded. No response was observed when identical concentrations of (*R*)-**3** (C) or (*S*)-**3** (D) were added to PqsD pretreated with ACoA. Furthermore, when (*R*)-**3** was added until saturation of the SPR signal, subsequent addition of (*S*)-**3** did not affect the observed response (E). The results indicate that the binding sites of both enantiomers are blocked by anthranilate.

11) Figure S10: Reversibility of PqsD inhibition by the Enantiomers (*R*)-3 and (*S*)-3

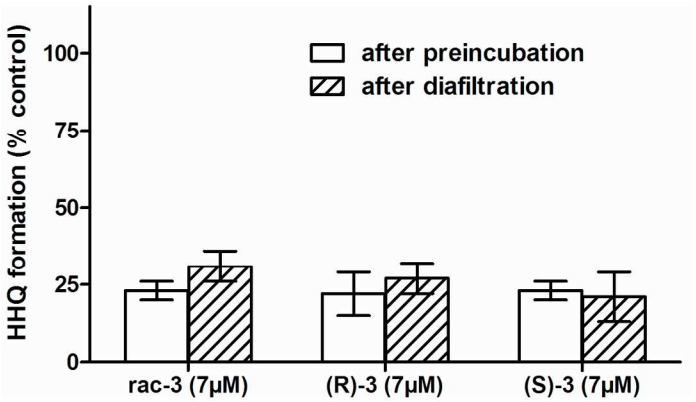

Figure S10. PqsD was preincubated with enantiomers (*R*)-**3** and (*S*)-**3** and the remaining HHQ formation was quantified with and without removal of unbound inhibitor by diafiltration. Centrifugal filter devices with a molecular weight limit of 10k were used to remove at least 95% inhibitor by three diafiltration steps as controlled by HPLC analysis, while PqsD was retained.

12) Representative ITC Curves

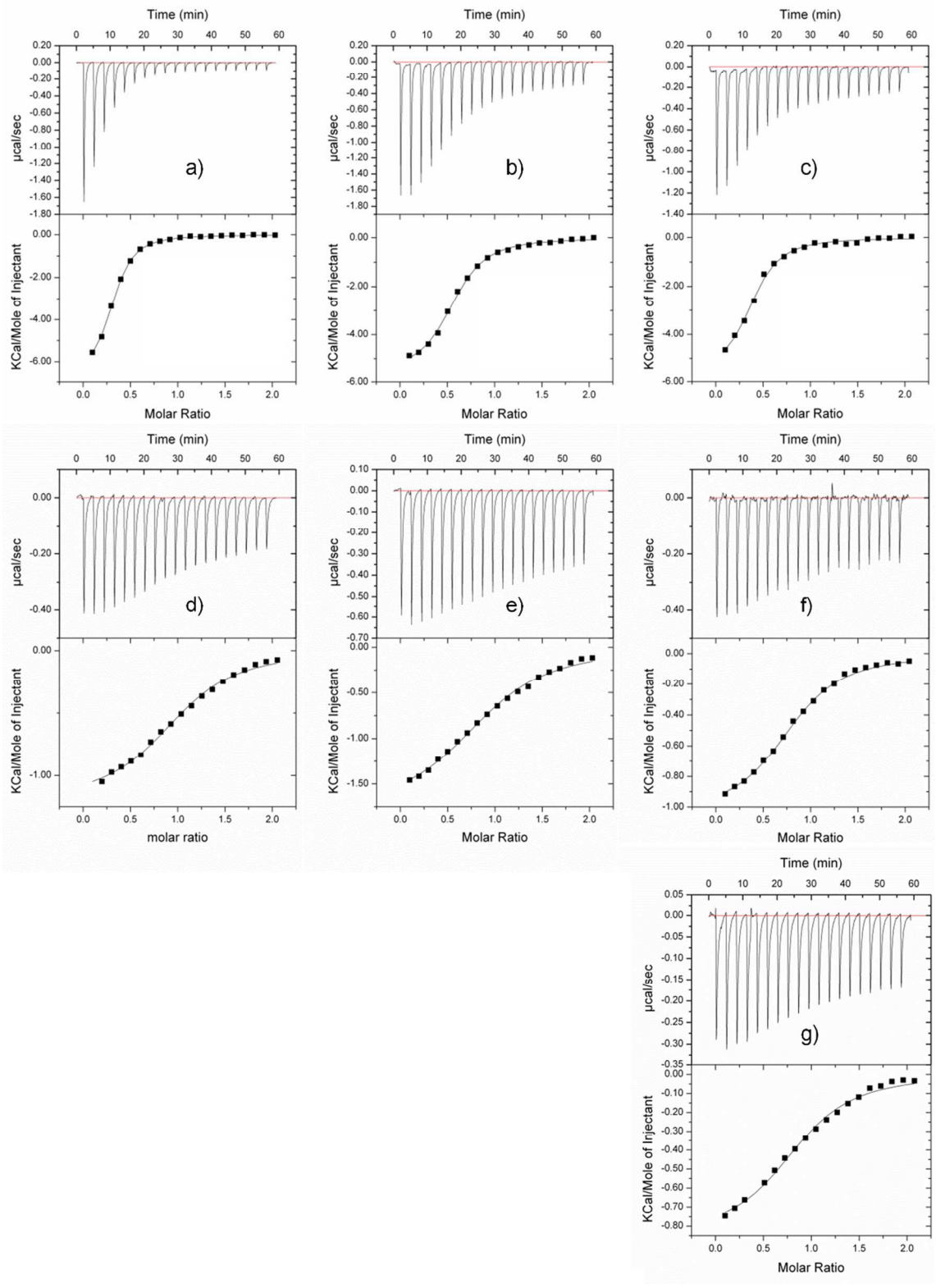

Figure S11 (above). Representative ITC titrations of *R*-enantiomer against PqsD wild-type and mutants. 3500 μM of compound against: a) PqsD wild-type (347μM), b) S317A (351μM), c) N287A (347μM), d) C112A (350μM), e) C112S (354μM), f) H257F (352μM), g) S317F (345μM). The recorded change in heat is shown in units of μcal sec^{-1} as a function of time for successive injections of the ligand (upper panel). Integrated heats (black squares) plotted against the molar ratio of the binding reaction. The continuous line represents the results of the non-linear least squares fitting of the data to a binding model (lower panel).

Figure S12 (below). Representative ITC titrations of *S*-enantiomer against PqsD wild-type and mutants. 3500 μM of compound against: a) PqsD wild-type (347μM), b) S317A (351μM), c) N287A (347μM), d) C112A (350μM), e) C112S (354μM), f) H257F (352μM), g) S317F (345μM). The recorded change in heat is shown in units of μcal sec^{-1} as a function of time for successive injections of the ligand (upper panel). Integrated heats (black squares) plotted against the molar ratio of the binding reaction. The continuous line represents the results of the non-linear least squares fitting of the data to a binding model (lower panel).

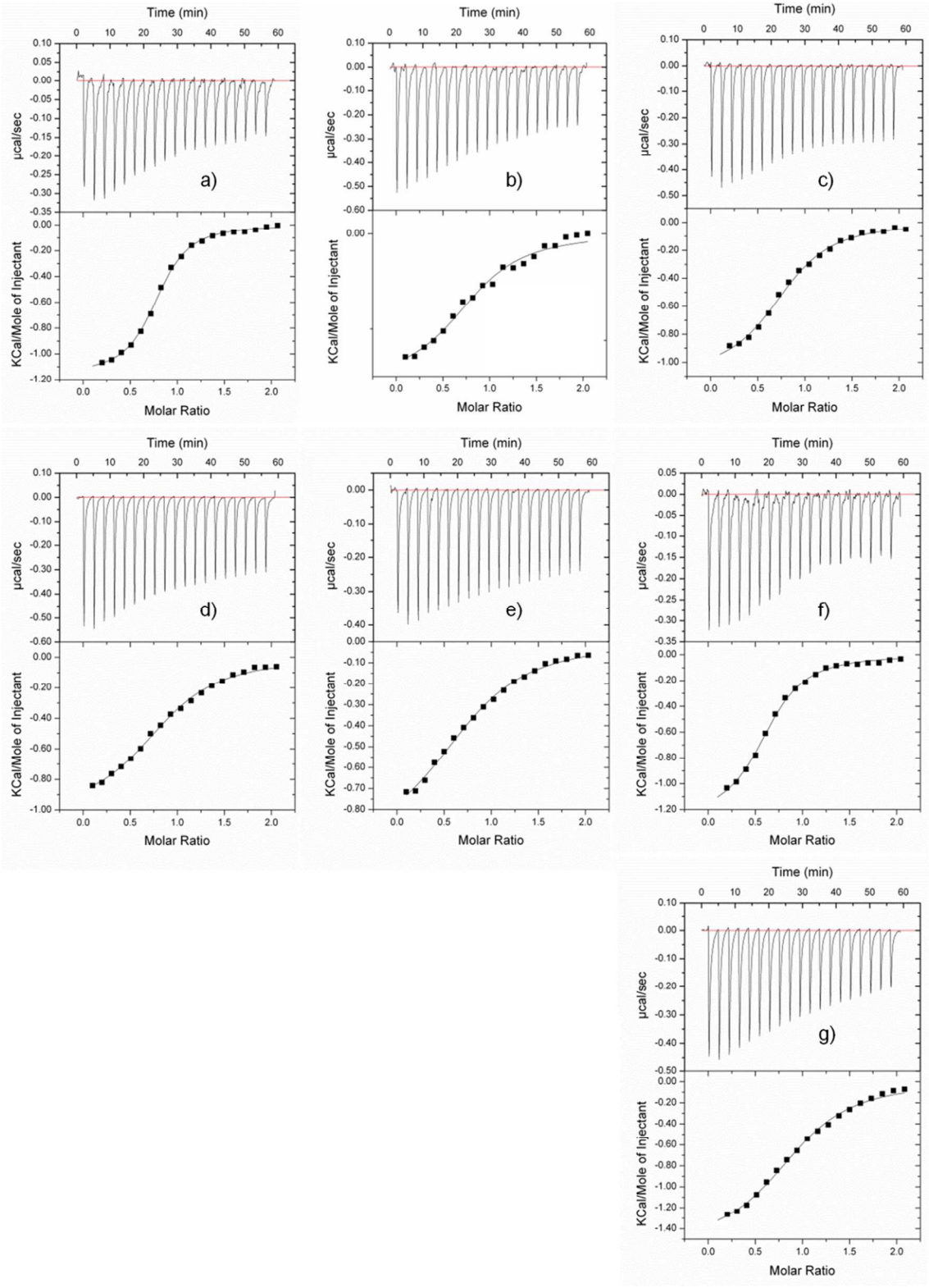
Time (min)
µcal/sec
KCal/Mole of Injectant
Molar Ratio
a)
b)
c)
d)
e)
f)
g)

13) References

SI1. Simon, E. J., Shemin, D. (1953) The preparation of *S*-succinyl coenzyme A, *J. Am. Chem. Soc. 75*, 2520.

SI2. Cook, L., Ternai, B., Ghosh, P. (1987) Inhibition of human sputum elastase by substituted 2-pyrones, *J. Med. Chem. 30*, 1017.

SI3. Nguyen, V. T. H., Bellur, E., Appel, B., Langer, P. (2006) Synthesis of 4-alkyl- and 4-(ω-chloroalkyl)-3-hydroxy-5-alkylidenebutenolides based on cyclizations of 4-alkyl- and 4-(ω-chloroalkyl)-1,3-bis(trimethylsilyloxy)buta-1,3-dienes with oxalyl chloride, *Synthesis 17*, 2865.

SI4. Geoghegan, K. F., Dixon, H. B. F., Rosner, P. J., Hoth, L. R., Lanzetti, A. J., Borzilleri, K. A., Marr, E. S., Pezzullo, L. H., Martin, L. B., LeMotte, P. K., McColl, A. S., Kamath, A. V., Stroh, J. G. (1999) Spontaneous *α-N*-6-Phosphogluconoylation of a "His Tag in *Escherichia coli*: The Cause of Extra Mass of 258 or 178 Da in Fusion Proteins, *Analytical Biochemistry 267*, 169.

SI5. Bera, A. K., Atanasova, V., Robinson, H., Eisenstein, E., Coleman, J. P., Pesci, E. C., Parsons, J. F. (2009) Structure of PqsD, a *Pseudomonas* quinolone signal biosynthetic enzyme, in complex with anthranilate, *Biochemistry 48*, 8644.

SI6. Duan, H.-F., Xie, J.-H., Shi, W.-J., Zhang, Q., Zhou, Q.-L. (2006) Enantioselective Rhodium-Catalyzed Addition of Arylboronic Acids to Aldehydes Using Chiral Spiro Monophosphite Ligands, *Organic Letters 8*, 1479.